Elsevier Editorial System(tm) for Journal of Materials Processing Technology

Manuscript Draft

Manuscript Number: PROTEC-D-07-00596

Title: Shaped Metal Deposition of a Nickel Alloy for Aero Engine Applications

Article Type: Research Paper

Keywords: Alloy 718; shaped metal deposition (SMD); microstructure; aerospace components

Corresponding Author: Dr Mark Whittaker, PhD

Corresponding Author's Institution: University of Wales Swansea

First Author: Daniel Clark

Order of Authors: Daniel Clark; Martin R Bache, PhD; Mark T Whittaker, PhD

Abstract: Manufacturing trials in support of shaped metal deposition (SMD) as a commercial process for the near net shape processing of aero-engine components are reported. Initially, relatively simple multi-pass linear weld deposition beads employing the nickel based polycrystalline superalloy Alloy 718 were characterized, to define the microstructural condition of the substrate and superimposed welds. Subsequently, a developmental combustion outer casing was fabricated via a hybrid-manufacturing route. This casing was formed from a forged ring with additive features, which included an internal, circumferential flange of Alloy 718, built up via an automated, high volumetric deposition rate MIG process. Under both circumstances, in the post deposition heat-treated condition (aged but not solution heat treated), the γ matrix contained laves micro-stringers, typically orientated parallel to the axis of epitaxy, with associated δ phase precipitation. On the micro scale, such micro-stringers were intimately associated with cracking or shrinkage porosity. Bi-axial stress fields imposed during the cooling of the large scale casing structure appear to influence the macroscopic organisation of these weld deposition defects.

PRIFYSGOL CYMRU ABERTAWE UNIVERSITY OF WALES SWANSEA

Yr Ysgol Beirianneg **School of Engineering**
Parc Singleton, Abertawe SA2 8PP Singleton Park, Swansea SA2 8PP

The Editor
Materials Science and Engineering A

30-3-07

Dear Editor,

Please find attached the submission of a research paper entitled "Shaped Metal Deposition of a Nickel Alloy for Aero Engine Applications" by Daniel Clark of Rolls-Royce plc, Martin Bache and Mark Whittaker of University of Wales Swansea. The work is original and has not been submitted for publication elsewhere. If there are any problems please contact myself (Dr Mark Whittaker) as the corresponding author, m.t.whittaker@swansea.ac.uk.
I look forward to hearing from you

Regards

Dr Mark Whittaker
Materials Research Centre
School of Engineering
University of Wales Swansea
SA2 8PP
Tel: +44 1792 295573
Fax: +44 1792 295693
E-mail: m.t.whittaker@swansea.ac.uk

Shaped Metal Deposition of a Nickel Alloy for Aero Engine Applications

D. Clark[#], M.R. Bache* and M.T. Whittaker*

[#] Rolls-Royce plc, P.O. Box 31, Derby, UK, DE24 8BJ

* Materials Research Centre, School of Engineering, University of Wales Swansea, UK, SA2 8PP

Abstract

Manufacturing trials in support of shaped metal deposition (SMD) as a commercial process for the near net shape processing of aero-engine components are reported. Initially, relatively simple multi-pass linear weld deposition beads employing the nickel based polycrystalline superalloy Alloy 718 were characterized, to define the microstructural condition of the substrate and superimposed welds. Subsequently, a developmental combustion outer casing was fabricated via a hybrid-manufacturing route. This casing was formed from a forged ring with additive features, which included an internal, circumferential flange of Alloy 718, built up via an automated, high volumetric deposition rate MIG process. Under both circumstances, in the post deposition heat-treated condition (aged but not solution heat treated), the γ matrix contained laves micro-stringers, typically orientated parallel to the axis of epitaxy, with associated δ phase precipitation. On the

micro scale, such micro-stringers were intimately associated with cracking or shrinkage porosity. Bi-axial stress fields imposed during the cooling of the large scale casing structure appear to influence the macroscopic organisation of these weld deposition defects.

Keywords

Alloy 718, shaped metal deposition (SMD), microstructure, aerospace components

Introduction

Aero gas turbine casings are designed to contain the gas stream through the compressor and turbine sections of the engine core. This involves the fabrication of annular structures offering the minimum of clearance between the internal casing wall and the rotating turbo machinery in order to optimize aerodynamic flow and thereby ultimate thrust and fuel efficiency. These structures invariably incorporate complex features such as flanges, open ports and bosses, necessary for joining sections of casing together or supporting peripheral components or control equipment. Given their complexity, casting has traditionally offered a suitable method for their manufacture. However, casing structures must also provide good structural integrity in the event of mechanical failure of the engine, i.e. they play a major role in containment. High strength properties are therefore essential, particularly to optimize design performance under high strain rates or impact. Cases manufactured from castings can be acceptable, however, these carry a weight penalty due to their less

consistent mechanical properties. Shaped metal deposition (SMD) has the inherent potential to outperform polycrystalline castings of the same chemistry in terms of mechanical properties, due to the more consistent solidification conditions made possible by a deposition process. The basic mechanical performance will be consistent for that seen in welds [1-7]. During normal service, load distribution is not even, therefore, hybrid forms, locally incorporating SMD properties [8] may be sufficient for features not subjected to primary pressure loading, subject to the agreement of the relevant engineering authorities. With an associated need for operation at elevated temperatures, forged nickel based super alloy casings are commonly employed with the annular form processed via methods such as ring rolling. Although the combination of mechanical working and specific heat treatment routines provides the optimum strength requirements, the forged component typically has to be manufactured substantially oversize to allow for final machining of the peripheral features. This can involve features which are difficult to forge such as boss pedestals or sharp changes in section. This induces added cost in terms of labour, tooling, reduced material yields and significant environmental implications [9].

Considerable research has been performed over recent years to retain the consistent, mechanical integrity benefits of ring rolled casing products whilst at the same time incorporating a near net shape philosophy. To this end, laboratory trials have been performed to assess the potential of SMD as a suitable technique for adding complex features to simple, relatively low stressed, substrate geometries. SMD typically involves increasing the thickness of material via localized, additive melting and solidification. The superposition of weld deposition beads is one technique that has received interest, largely

due to the fact that the method can employ standard welding equipment without the need for extensive new investment. Previous workers at Rolls-Royce including the present authors have investigated SMD using TIG deposition and lasers as deposition heat sources with various consumable forms. Other workers have also investigated variants of these [10] and also the use of an electron beam as a heat source for deposition [11]. While these deposition processes have individual characteristics and limitations, there are commonalities. In order to achieve a high volumetric build rate, there are considerations of pool size and process velocity when designing a process which can practically and economically produce material to an acceptable level. So as to consider the effectiveness of a robust mechanised system, using where possible standardised equipment, metal inert gas (MIG) deposition was selected for the present study. It was considered that MIG welding could offer an attractive, high deposition rate to make the SMD process economically viable. MIG offers high power densities at low cost, while the use of a synergic control relationship allows a practical form of process control at rapid processing rates. In common with SMD techniques utilising TIG, lasers and electron beams linked to wire feed systems, the use of a consumable electrode offers a standard consumable form, with a particular advantage for additive manufacture of more consistent feed angles. The MIG process can be pulsed, doubled-up as a tandem deposition using a single automation system and hybridized, using a laser to control weld pool fluidity and solidification dynamics (for example influencing wetting behaviour around the pool perimeter and marangoni flow). These considerations are particularly important when considering direct manufacture of large scale components. Wire based deposition offers further advantages in terms of material utilization relative to competing powder based techniques. In the first instance,

however, detailed characterisation of MIG depositions was required to establish the controlling process parameters to ensure optimum weld structures.

This detailed microstructural study builds on a previous project, which provided initial characterisation of Alloy 718 SMD structures in terms of alloy chemistry and a limited mechanical property assessment [12]. The current research employed a two stage investigation. Initial trials were performed to lay down straight line single stringer / multiple layer (SS/ML) weld deposition beads on a flat forged plate substrate of Alloy 718 using a consumable Alloy 718 electrode. The welds and the substrate were subjected to detailed metallographic inspection to identify the resulting metallurgical phases and microstructural condition [13, 14]. Subsequent to these findings, supplementary manufacturing trials were completed to develop the automated deposition of more complex geometries such as multi stringer / multi layer cylinders. This culminated in the fabrication of a SMD developmental ring rolled combustor casing structure which incorporated a number of additive features including an internal SMD / MIG flange. The SMD flange, containing a double stringer / multi layer architecture, was then subjected to detailed microstructural inspection and compared to the original findings.

Although the present paper deals with the specific example of casing structures, SMD processes offer potential towards the manufacture or repair of many aero-engine components. The implications of the current work for the wider application of SMD techniques will be discussed.

Experimental Methods

General Welding Parameters

All the SMD structures were laid down using a computer controlled Synergic MIG power source under robotic guidance [15]. Aerospace grade material stocks for the Alloy 718 consumable electrode and substrate were employed. Argon gas was used as a local shrouding media without any additional environmental shielding. Extensive trials had previously optimized the key control parameters to produce repeatable, single pass depositions: i.e. synergic relationship, process gas, voltage, travel speed, wire feed rate, torch angle and stick-out (the distance between the lowest point of the welding torch and the work piece). This was accomplished using design of experiment (DoE) multi-variable analysis [16] based on deposition profile and optical microscopy [17]. The criteria for weld optimisation had included fusion (wetting angle/undercutting), spatter, deviation from a straight line [18], bead height and width, substrate penetration and defect content (porosity or cracking [19]). The optimized parameters were derived as per a normal cladding process but with specific additional constraints. These constraints were imposed due to the different heat flux (due to varying substrate temperatures and topography) and microstructural requirements. Note that the microstructural requirements were based on criteria for the as-deposited material, the interfacial fusion region and the parent (substrate). These criteria also covered the post-deposition heat-treated micro-structures. A comprehensive

metallographic examination of representative deposition geometries in various locations and orientations was performed as a part of the validation trials.

Metallographic Sectioning

Metallographic specimens were mounted in conductive bakelite, polished using standard grinding techniques, and underwent a final chemical polish with an aqueous suspension of colloidal silica containing 20% H_2O_2 (Hydrogen Peroxide). Subsequently, specimens were etched with a solution of 10ml HNO_3, 20ml HCl, 25ml distilled water and 10ml hydrogen peroxide (H_2O_2) for approximately 150 seconds. Microstructural analysis was performed on both a Jeol 6100 SEM and Phillips XL30CP SEM. Chemical analyses were performed using a Jeol-35C SEM fitted with an Oxford Instruments EDX X-ray dispersion facility.

Deposition trials

Straight Line Single Stringer / Multiple Layer depositions

Multiple pass weld beads were laid down to increase the height of a straight line deposit. The control parameters for single pass weld deposits, as described in Table I, were fixed during each layer of deposition. This essentially fixed the amount of energy supplied during each deposition pass, therefore, a new parameter, delay time between depositions, required further optimisation. An understanding of the heat build up during successive deposition operations, related to substrate temperature, was important since adverse effects on

solidification dynamics could occur [20-30]. Solidification rate affects the microstructural condition, wetting angle of the beads, bead cross sectional depth, fusion profile and residual stresses. Control of the pool geometry, whether essentially elliptical or teardrop [31, 32] and the rate of solidification (indicated by dendrite arm spacing measurement) primarily influenced segregation [33-35]. The degree of segregation and solidification dynamics controlled the distribution of carbon-rich and topographically close packed (TCP) phase distribution. Relatively fast freezing and cooling to a low temperature after the most recent weld deposition will discourage grain growth [36] in the underlying substrate or deposition beads and avoid secondary precipitation [37]. These are seen as beneficial effects particularly with reference to the eventual high temperature mechanical properties of the material. On the other hand, rapid cooling may encourage high residual stresses across the width of the weld [38, 39], promoting hot tearing during solidification [40] or post solidification cracking [41]. The control of heat flux is considered a key parameter, influencing internal stresses and component distortion and affecting the consistency of welding.

The delay time between depositions was optimized for a given geometry in order to provide a maximum interpass deposition bead temperature of approximately 80^{o}C (measured using thermocouples brought into contact with the solidified as-deposited surface). The interpass cooling regime was a balance based on the build parameters requiring a consistent cooling rate for microstructure and side-wall profile against the induced stresses from the sharp temperature differential. High rate deposition can otherwise allow a significant build up in thermal mass, which can risk an adverse precipitation response. Clearly, the ability to

perform this interpass interval when producing larger SMD structures would be highly dependent on the speed of positional control offered by the robotic welding/deposition facility. A schematic example of single string / multiple layer weld deposition geometry is illustrated in Figure 1.

Straight Line Double Stringer / Single Layer Depositions

In order to increase the overall width of any deposited structure, parallel, multiple stringer welds are often required. However, from the point of view of metallurgical control, it is preferable to fabricate such structures from repeatable "building blocks" of consistent geometry and associated microstructural detail. Therefore, during the present study, emphasis was placed on the validation of a specific "voxel" section [42]. Hence, a voxel parameter set was developed, which produced a consistent, cross sectional profile and internal microstructure. This imposed strict bounds to the geometrical range of validation for the build element. Over and above the control parameters optimized previously for single stringer depositions, two new parameters required consideration for the formation of multiple stringers on a common plane, namely the distance between adjacent weld deposition beads (or overlap) and the time interval between consecutive passes. Referring to Figure 2, the average single weld deposition bead width (i.e. twice the weld pool radius) during the present trials was set to 12.8 mm. The optimum distance between parallel weld deposition beads, from the microstructural and defect viewpoint, was found to be 6 mm, providing an overlap of 6.8 mm. A schematic example of double stringer weld deposition bead geometry is illustrated in Figure 3. The delay time between adjacent welds was

eventually set to 2 minutes. It should be appreciated that in practice there will be allowable tolerances placed on such variables.

Straight Line Double Stringer / Multiple Layer Depositions

The final plate trials on straight line depositions combined all of the previous experience to form double stringer / multiple layer weld deposition bead deposits. The optimized parameters for single weld deposition beads were employed throughout. The time delay between adjacent weld deposition beads was set to 2 minutes, with 10 minutes delay between each layer. An example of a double stringer / six layer deposit is illustrated by the orthogonal section (X-Z plane) in Figure 4. Evidence of the weld stacking is obvious on the peripheries of this early stage example, probably as a result of the variable geometric heat sink as the deposit grew in volume. Although such flank features were subsequently minimized through process optimization, they would typically require final machining to eliminate stress-raising features as sites of potential service cracking [43]. Weight is also a consideration for aerospace, so volumetric excess may be removed for this reason alone.

In general, the resulting microstructure after heat treatment consisted of a γ matrix with γ" and laves "micro-stringers" (note this term is used throughout to describe the microscopic form of the internal laves structures and should not be confused with "stringers" typically used in the literature to describe macroscopic weld beads) [44-47]. When viewed in the X-Z plane, these micro-stringers were essentially parallel to the axis of epitaxy, Figure 5a, but rafted in an interlocking structure in the X-Y plane, Figure 5b. Co-incident with the laves

were fine scaled δ phase needles, Figure 6. Overlay intervals longer than the optimum 10 minutes notably encouraged "fissures" in the vicinity of the overlap region, i.e. on the macroscopic scale vertically along the centre of the orthogonally sectioned welds. The approximate location, orientation and extent of these features are indicated in Figure 4. It was significant that these fissures never extended into the final uppermost layer, suggesting they were the result of re-heating of previous weld layers. All the fissures were intimately related to the dominant laves micro-stringers. However, whereas under some circumstances they appeared as angular crack like discontinuities, Figure 7, more often than not they took an elongated porous appearance, Figure 8. The temporal relationship between the laves and the fissures was confirmed through a series of subsequent heat treatment trials. Laves are considered to form during extensive time at relatively high temperature. By heat treating specimens containing pre-existing cracks no further formation of laves occurred along the flanks of the fissures, indicating that during welding, the laves must have pre-dated the cracks or pores.

SMD Cylinders

A series of experimental cylindrical structures were also produced spanning single stringer / single layer, double stringer / single layer, single stringer / multiple layer and finally double stringer / multiple layer morphologies. A schematic example of such structures is illustrated in Figure 9. An added complication of these structures is the localized overlap and associated reheating at the start–stop location of individual cylindrical deposition rings. In addition, minor differences in the relative speeds of deposition are experienced on the outer

and inner walls of the circular weld bead. This radial variation manifested itself as a variation in rate of heat loss and visually as a change in surface finish. Despite these factors, the macroscopic finish and metallographic condition of these cylinders essentially replicated the straight welds. The exercise proved to be a useful step prior to the fabrication of more complex three dimensional structures including casing bosses and the internal compressor casing flange to be described in detail below.

Developmental Combustor Outer Casing – SMD Internal Flange

Technical trials to assess the suitability of SMD for additive component manufacture have included the fabrication of a developmental (i.e. intended for ground testing only) Alloy 718 ring rolled combustion casing incorporating an internal, circumferential SMD flange. The flange was composed of a double stringer / multiple layer (DSML) series of overlaying, circumferential MIG weld deposition beads built up via automated, robotic control. The key parameters controlling deposition of the MIG (argon) SMD structure are presented in Table II. Sixteen layers were required to build the flange to the requisite height. Subsequent machining operations removed the surface material from the weld beads to produce a final casing flange to typical specification. The entire casing was then subjected to a post deposition heat treatment, a check for distortion, a two stage ageing treatment and finally machined to tolerance.

It is emphasized at this point that a solution or homogenization heat treatment may be preferred to optimise the specific microstructure of the SMD material. In the hybrid route

however, consideration must be given to the effects of this heat treatment on the substrate component, both metallurgically and in terms of machined geometries (i.e. distortion). Even if substrate microstructures were substantially unaffected, for example via a localised thermal treatment with precisely controlled zones for the steady state isotherms, residual stress re-distribution and distortion of the finished form could result.

At this stage, chord segments from the SMD flange were extracted from the casing, Figure 10, by machining through the thickness of the flange adjacent to the junction with the internal casing wall/pedestal via a conventional turning operation. These were then cropped to suitable size for mounting and metallurgical polishing. The original SMD lay-up, flange machining operation, extraction of the chords and their relationship to the casing / SMD geometry are all illustrated in the sequence of schematic illustrations in Figures 11 and 12. A single reference system was employed to describe the orientation of the specimens and their internal structure. The direction of SMD build up, equivalent to the radial axis of the combustion casing, was designated the Z axis; the hoop direction of the casing or flange the Y axis; and finally the longitudinal axis of the annulus casing the X axis.

In general, the microstructure within the SMD flange, when viewed at high magnification, was identical to the welding trials previously described, i.e. a γ matrix containing γ' and laves micro-stringers orientated parallel to the direction of epitaxy plus associated δ phase needles [12]. However, extensive sinuous cracking was also noted during low magnification optical inspection, even prior to chord removal. This was best illustrated after polishing and etching the Y-Z plane and demonstrates that the cracking transects the

multiple weld beads, Figure 13. The orientation of these macro scale cracks appears to be influenced by the post weld bi-axial stress field imposed during cooling. In the Y-Z plane, contraction in both the radial and hoop orientations would be constrained by the surrounding casing. The resultant principal tensile stresses appear to be orientated at approximately 45^{o} to either axis, inducing the tortuous nature of the cracking.

However, at higher magnifications the local control of crack path was clearly due to the weld microstructure, particularly regions of dense laves precipitation. In addition, alternative paths for the discontinuity were offered by shrinkage porosity within the flange, especially in the overlaying weld zones. Laves structures tended to form in regions of concentrated chemical segregation, therefore, future research should focus on minimizing such segregation effects during thermo-mechanical processes. The main causes of segregation are the freezing dynamics of the weld pool, hence pool size, shape, depth and the substrate temperature. Where additive manufacture differs from single pass welding is in the various orientations of the temperature gradients and the degree of remelting (which can concentrate segregates in a manner similar to weld pool centreline segregation). Mitigation strategies can take the form of varying the tool path and deposition fill-patterns. These SMD techniques can also assist in maintaining level height over successive layers. Efforts to correlate laves and associated crack orientations to potential microtexture within the weld deposits, were undertaken by matching dendrite arm orientations relative to the laves. Such lattice texture could be acquired from the epitaxy resulting from thermal gradients. However, no clear orientation preferences were noted.

Since volumetric non destructive evaluation (NDE) of the as welded SMD flange had not been performed prior to this stage of the manufacturing sequence and no samples were available from the as welded flange prior to machining, it can not be confirmed whether the mechanical removal of surface material and associated machining induced residual stresses were pre-requisites for the introduction of the cracking or whether these features are solely a result of the PDHT processes.

Discussion

The current trials have demonstrated the potential of SMD technology in the fabrication of complex engineering structures. Within the aerospace sector, the near net shape capability of additive SMD should offer obvious benefits in terms of improved materials yield and a reduction in mechanical surface removal operations – both key factors controlling the cost of individual components. SMD provides a relatively rapid manufacturing process for large scale features and can be automated through efficient multi-axis and multi-arm robotic controlled welding systems.

However, detailed consideration must be given to the ultimate metallurgical and microstructural condition evolved during SMD manufacture. In particular, the present study has highlighted the presence of deleterious phases within the Alloy 718 MIG weld deposition structures (i.e. relatively brittle laves and δ phase segregation encouraged by extended time at high temperature during either deposition, through the cumulative

exposure to transient deposition, or subsequent Post Deposition Heat Treatment (PDHT)). The present study has confirmed previous reports [25, 35], noting that these phases evolve in preferred orientations, potentially inducing an anisotropic mechanical response under subsequent loading. Volumetric changes associated with phase transformation may also have a local shearing effect across interfaces. In addition, associated discontinuities in the form of cracks and shrinkage porosity have been identified. In DS/ML weld deposition structures, the degree of reheating introduced during overlay operations appears to be critical for controlling the introduction of these defects [12, 45, 46]. However, despite systematic optimization of the major weld control parameters such features persist. This may prove to be a significant limitation in considering MIG for aerospace applications. Added to this, the adverse effects of residual stress have also been demonstrated (affected during either machining or PDHT operations) through the introduction of macroscopic cracking in this feature of the demonstrator casing component.

For high integrity components in aero gas turbines subjected to relatively demanding loading regimes, such phases as laves and delta must either be eliminated through precise thermo-mechanical processing or otherwise demonstrated to be "benign" under typical service conditions (i.e. the component demonstrates sufficient "phase tolerance" and resists the formation of a critically sized crack from a pre-existing flaw over a specified period of operation). Given this philosophy, the major engine manufacturers appear to be adopting consistent strategies for additive manufacture (AM), restricting the techniques' potential use to non critical component locations at this stage of process maturity [48]. Even in the present example of the developmental combustor casing, the SMD flange was designed as

an additive feature upon an internal wall pedestal, ensuring the flange itself would not experience design limiting hoop stresses. However, casing structures routinely experience at least one major fatigue cycle per flight; the thermal-mechanical cycle imposed during normal engine use and shut down. High cycle fatigue may also be superimposed as a result of vibration. Therefore, improvements in additive technologies to avoid the introduction of crack initiating defects would clearly be advantageous. It is unlikely that MIG based SMD used for hybrid near net shape components without a homogenisation treatment can eliminate the laves phase formation, due to the restrictions on pool size and hence the influence on freezing rate and segregation. To this end, methods of metal deposition, having smaller volumetric build unit sizes, may prove more suitable for the manufacture of higher integrity components. By controlling the build up of material on the microscopic scale (for example individual molten "pools" may be less than a millimetre diameter with some AM techniques) any incipient porosity, the evolving grain size and the internal microstructure are all fundamentally smaller. The resultant volume of material should also demonstrate more homogeneous mechanical properties and any long range residual stresses minimised. Macro-scale demonstration components are currently under manufacture for future detailed characterization, Figure 14.

Conclusions

From the practical viewpoint, the current research has demonstrated that SMD processes generally provide a viable method of fabricating local, complex features in aerospace components. The ultimate microstructural condition of these features is, however, highly

dependent on welding deposition parameters and practice. In the specific case of Alloy 718, it has been shown that phases such as laves and delta, deleterious to mechanical properties, may form through localised chemical segregation. The cooling rate in particular must be controlled to avoid such phases, with fast freezing and minimal re-heat favoured throughout the process history. Careful consideration of residual stresses imparted during fabrication and subsequent service loading is also required.

Cracking in this alloy system is well documented. As new techniques for material volumetric forming are developed, corresponding process rules and models are required to ensure sound processing. The cracks seen in this instance were closed and present in bulk material with comparatively large microstructural features relative to forgings, as such they were not evident until close to completion of the manufacturing route. In consideration of this type of flaw, it is important that appropriate volumetric inspection techniques are concurrently developed.

Continued research is required to establish generic microstructural acceptance standards for this specific alloy, together with alternative nickel and titanium systems, which relate to these techniques of high rate, weld deposition.

REFRENCES

[1] Roberts, S.M., Hunziker, O., Dye, D., Reed, R.C., "The development of a process model for the weldability of nickel-base superalloys for gas turbine applications. Life Assessment of Hot Section Gas Turbine Components", Proceedings of Conference, Edinburgh, UK, 5-7 Oct.1999. Ed: Townsend, R., Winstone, M.,

Henderson, M., Nicholls, J.R, Partridge, A., Nath, B., Wood, M. and Viswanathan, R. Book B731. Publ: London, SW1Y 5DB, UK; IOM Communications Ltd (The Institute of Materials), pp.327-337, (2000).

[2] Lingenfelter, A.C., Welding Metallurgy of Nickel alloys in Gas Turbine Components, Joining and Repair of Gas Turbine Components, 15-18 September 1997, Conference Proceedings from Materials Solutions '97, ASM International 1997.

[3] ASM Handbook, Volume 6, "Welding Brazing and Soldering", ASM International, 1993.

[4] Lampman, S., (Editor) Weld Integrity and Performance, Chapter 17 – Properties of Nickel-Alloy Welds, ASM International, 1997.

[5] Betteridge, W., Heslop, J., "The Nimonic alloys and other Nickel-Base High Temperature Alloys", Edward Arnold (Publishers) Ltd., 1974.

[6] Donachie, M.J., Donachie, S.J, "Superalloys, A technical guide", ASM International, 2002.

[7] Hoback, G.L., Britton, M.A., Diedrick, D.F., "Weldability of High Temperature Alloys in Thick Sections. Joining and Repair of Gas Turbine Components", 15-18 September 1997, Conference Proceedings from Materials Solutions '97, ASM International, 1997.

[8] Mills, W.J., Fracture Toughness Variations for alloy 718 Base Metal and Welds, Superalloy 718 – Metallurgy and Applications, The Minerals & Materials Soc., (ed. Loria, E.A) pp. 517-532 (1989).

[9] Clark, D., Allen, J., Rapid Manufacturing of Aerospace Structural Components, Time Compression Technologies Conference, TCT 2006.

[10] Blackwell, P.L., "The mechanical and microstructural characteristics of laser-deposited IN718", Journal of materials processing, vol. 170, n°1-2, pp. 240-246, 2005

[11] Matz, J.E., Eagar, T.W. Carbide Formation in Alloy 718 During Electron Beam Solid Freeform Fabrication. accepted by Metall. Trans., (2002).

[12] "Metallographic Characterisation of IN718", Swansea UTP, report to Rolls-Royce, 2003.

[13] Durand-Charre, M., The Microstructure of Superalloys, CRC Press, (1997)

[14] Carlson, R.G., Radavich, J.F., Microstructural Characterisation of cast 718. Superalloy 718 – Metallurgy and Applications (ed. Loria, E.A), The Minerals & Materials Soc., pp. 79-93 (1989).

[15] Jiluan, P., Arc Welding Control, Woodhead Publishing Ltd, (2003)

[16] Anthony, J., Design of Experiments, For Engineers and Scientists, Elsevier Butterworth-Heinemann, (2003)

[17] Pandrey, S., Parmar, R.S., Mathematical Models for Predicting Bead Geometry and Shape Relationships for MIG Welding of Aluminium Alloy 5083. Recent Trends in Welding Science and Technology Edited by David, S.A., and Vitek, J.M., ASM International (1990).

[18] Wheeler, J.D., Understanding Variation, the Key to Managing Chaos, SPC Press, Inc, (1993)

[19] Yeniscavich, W. Joining, Superalloys II, High Temperature Materials for Aerospace and Industrial Power, Edited by: Sims, C.T., Stoloff, N.S., Hagel, W.C., Wiley-Interscience., (1987)

[20] DuPont, J.N Solidification and Weldability of Nb-Bearing Superalloys. Welding Journal , 77(10):417-431, (1998).

[21] Bouse, G.K., Application of a modified phase diagram to the production of cast alloy 718 components, Superalloy 718 – Metallurgy and Applications (ed. Loria, E.A), The Minerals & Materials Soc., pp. 69-77 (1989).

[22] Knorovsky, G.A., Cieslak, M.J., Headley, T.J., Romig, A.D., Hammetter. W.F., Inconel 718: A solidification diagram, Metallurgical Transactions A, vol. 20A, pp. 2149-2158 (1989).

[23] Cieslak, M.J., Knorovsky, G.A., Headley, T.J., Romig Jr, A.D., Kollie, T., The Solidification Metallurgy of Alloy 718 and other Nb-Containing Superalloys, Superalloy 718 – Metallurgy and Applications, The Minerals & Materials Soc., (ed. Loria, E.A) pp. 59-77 (1989).

[24] Cieslak, M.J., Headley, T.J., Knorovsky, G.A., Romig Jr, A.D., Kollie, T., A comparison of the solidification behaviour of Incoloy 909 and Inconel 718, Metallurgical Transactions vol. 21A, pp. 479-488 (1990).

[25] Cieslak, M. J.; Knorovsky, G. A.; Headley, T. J.; Romig, A. D. Jr., "Use of new PHACOMP in understanding the solidification microstructure of nickel base alloy weld metal", Met. Trans. A, 17(12), 1986, pp 2107-2116.

[26] Park, J.W., Vitek, J.M., Babu, S.S., David, S.A., Stray Grain Formation, Thermomechanical Stress and Solidification Cracking in Single Crystal Nickel Base Superalloy Welds, Science and Technology of Welding and Joining, Vol.9. No. 6. (2004)

[27] Dye, D., Hunziker, O., Reed, R. C., Numerical analysis of the weldability of superalloys. Acta Materialia, vol.49, no.4... pp.683-697 (2001)

[28] Perricone, M.J., DuPont, J.N., Weld Solidification Behaviour of Superaustenitic Stainless Steel and Ni-Base Alloys, Proceedings from Joining of Advanced and Specialty Materials, 7-9 October 2002, Columbus, OH, ASM International, (2003).

[29] Lampman, S., (Editor) "Weld Integrity and Performance", Chapter 1 – Weld solidification, ASM International, 1997.

[30] Park, J.W., Vitek, J.M., Babu, S.S., David, S.A., "Stray Grain Formation, Thermomechanical Stress and Solidification Cracking in Single Crystal Nickel Base Superalloy Welds", Science and Technology of Welding and Joining, 2004, 9(6).

[31] Hunziker, O; Dye, D; Reed, R.C., On the formation of a centreline grain boundary during fusion welding. Acta Materialia, vol.48, no.17. pp.4191-4201 (2000)

[32] Tillack, D.J. "Nickel alloys and stainless steels for elevated temperature service: weldability considerations", Proceedings from Materials Solutions '97 on Joining and Repair of Gas Turbine Components. ASM International, Indianapolis, Indiana, USA1997.

[33] Fleming, M.C. "Solidification Processing", McGraw Hill Book Company, 1974.

[34] Sindo, K., Welding Metallurgy 2nd Edition., Wiley-Interscience., (2002)

[35] Jones, S.M., Radavich, J., Tian, S., Effect of Composition on Segregation Microstructures and Mechanical Properties of Cast Alloy 718, Superalloy 718 – Metallurgy and Applications, The Minerals & Materials Soc., (ed. Loria, E.A) pp. 589-598 (1989).

[36] McLean, D. Grain Boundaries in Metals, Oxford, Clarendon Press, (1957).

[37] Vincent, R., Precipitation around welds in the nickel-base superalloy, Inconel 718, Acta Metallurgica, vol.33, no. 7, pp. 1205-1216 (1985).

[38] Dye, D., Roberts, S.M., Withers, P.J., Reed, R.C., The determination of the residual strains and stresses in a tungsten inert gas welded sheet of IN718 superalloy using neutron diffraction, Journal of Strain Analysis, vol. 35 No.4 (2000)

[39] Ma, S., Rangaswamy, P., Majumdar B.S., Microstress evolution during in situ loading of a superalloy containing high volume fraction of γ' phase Scripta Materialia 48 (2003) 525–530

[40] Thompson, R.G., Genculu, S., Microstructural Evolution in the HAZ of inconel 718 and Correlation With The Hot Ductility Test. Welding Journal , 62(12):337-345, December (1983)

[41] Dye, D., Mechanical Effects Arising From the Welding of Superalloys, Dissertation for the Degree of Doctor of Philosophy, University of Cambridge, (September 2000).

[42] Degarmo, E.P., Black, J.T., Kohser, R.A., "Materials and Processes in Manufacturing", 9th Edition, John Wiley, 2003.

[43] Bache, M. R., Evans, W. J. and Hardy, M.C., "The effects of environment and loading waveform on fatigue crack growth in Inconel 718", International Journal of Fatigue, vol 1, supplement 1, Pages 69-77 (September 1999)

[44] Qiang, Lu., Lippold, J.C., R Bowers., Alloy 718 Heat Affected Zone Microstructural Evolution after Multiple Repair and Postweld Heat Treatment Cycles., EWI CRP Summary Report SR0111, (2001)

[45] Bowers, R, Hooijmans, J., Lippold, J.C., Effect of Composition and Heat Treatment Cycles on the Repair Weldability of Alloy 718, Joining and Repair of Gas Turbine Components, 15-18 September 1997, Conference Proceedings from Materials Solutions '97, ASM International, 1997.

[46] Qian, M., Lippold, J.C., The effect of rejuvenation heat treatments on the repair weldability of wrought Alloy 718, Mat. Sci.Eng., A340, 2003, pp 225-231.

[47] Qian, M., Lippold, J.C., The effect of annealing twin-generated special grain boundaries on HAZ liquation cracking of nickel-base superalloys, Acta Materialia 51 (2003) 3351–3361

[48] Kinsella, M.E., Additive Manufacturing for Aerospace Applications, Welding in Aircraft and Aerospace Conference, September 19-20, AWS 2006.

Figure 1
Click here to download high resolution image

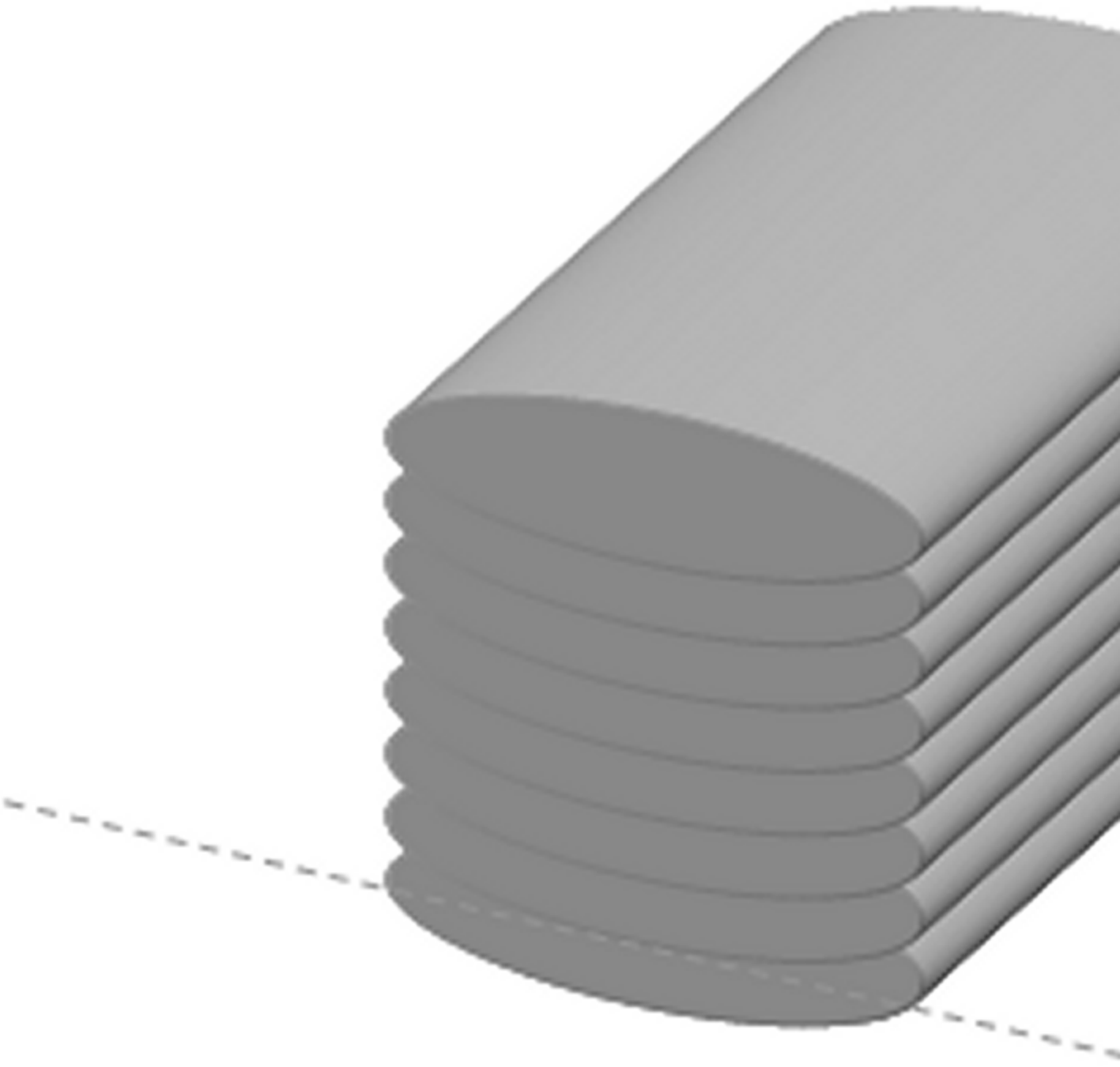

Figure 2

Click here to download high resolution image

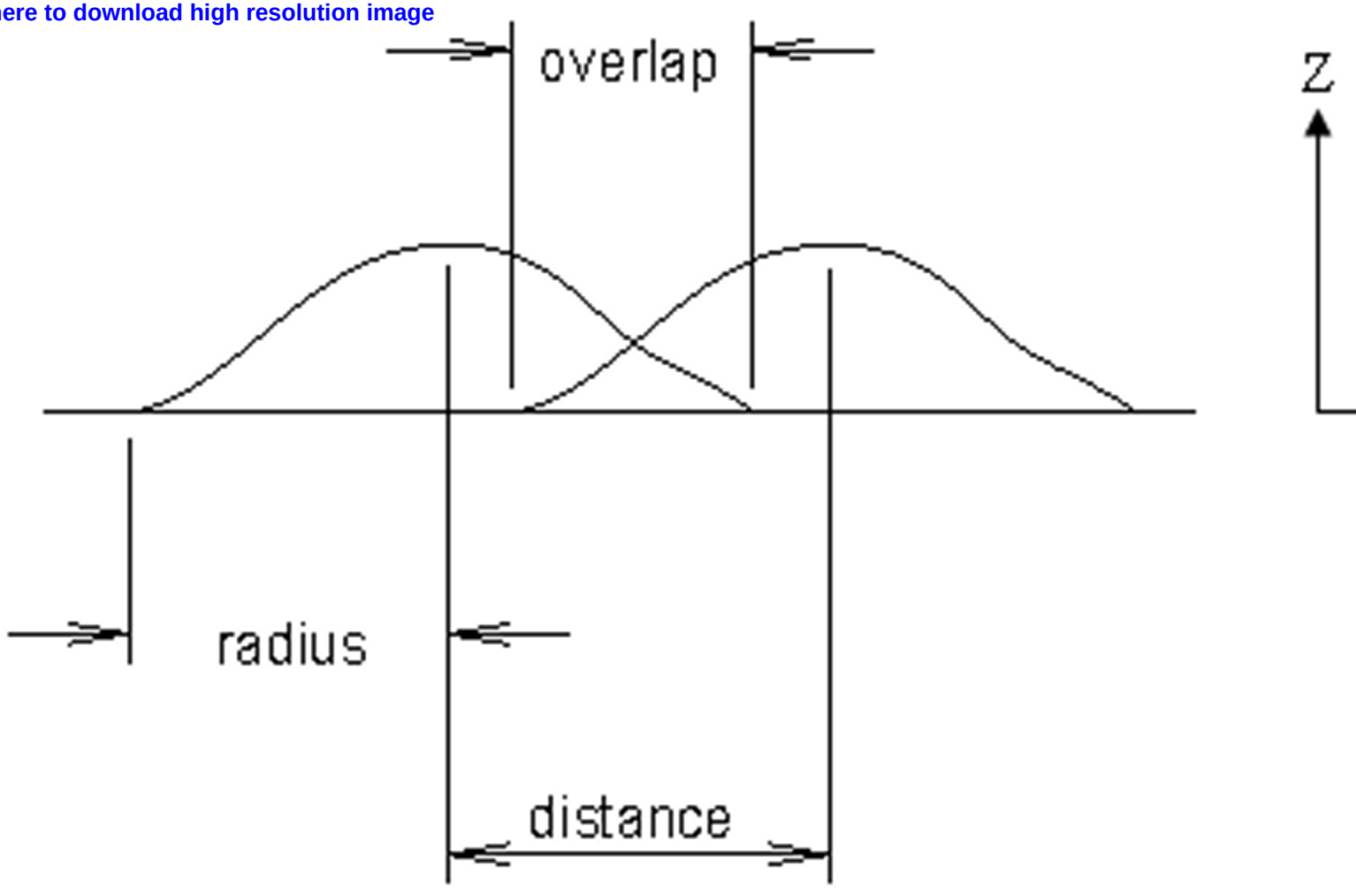

Figure 3

Click here to download high resolution image

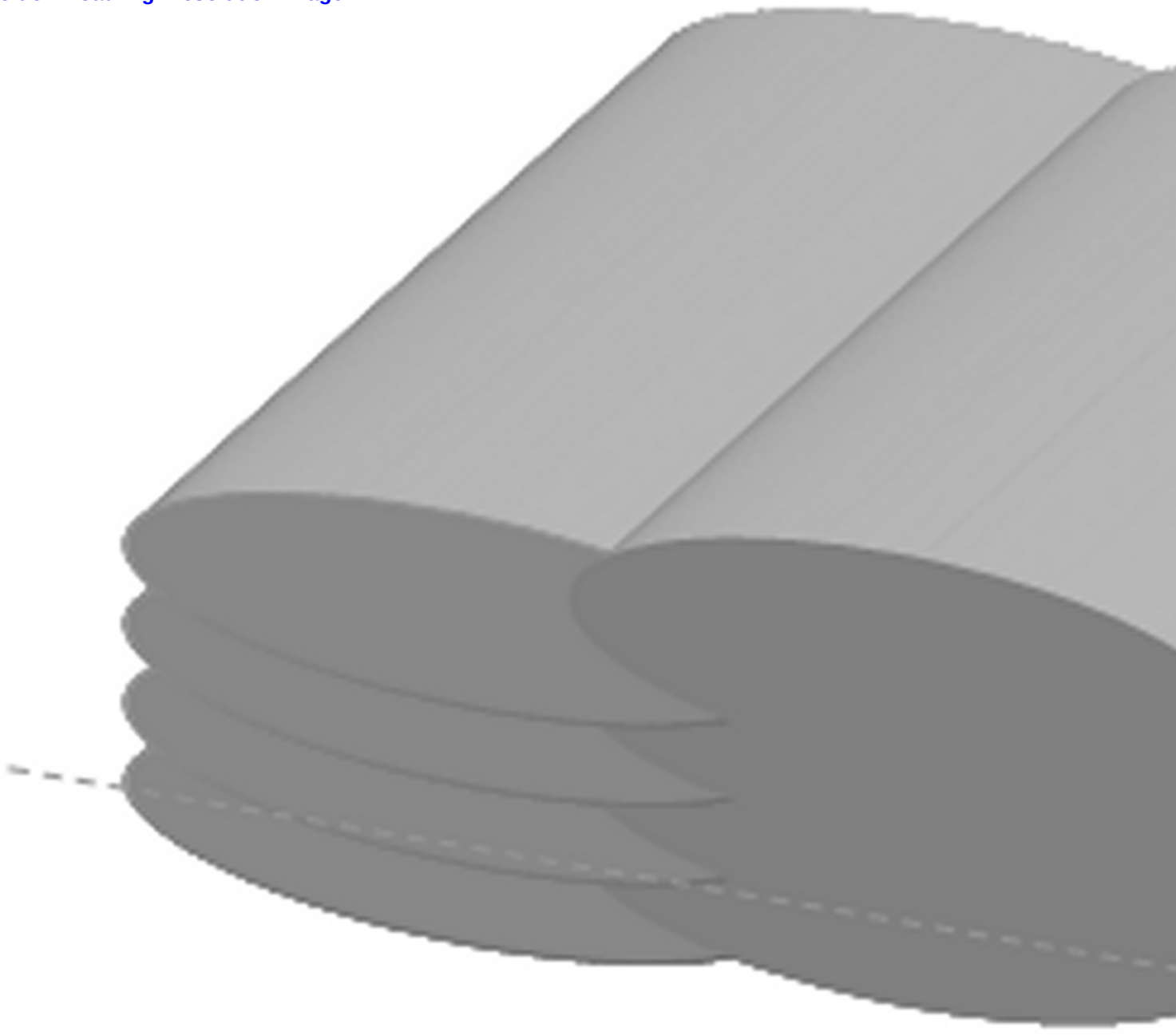

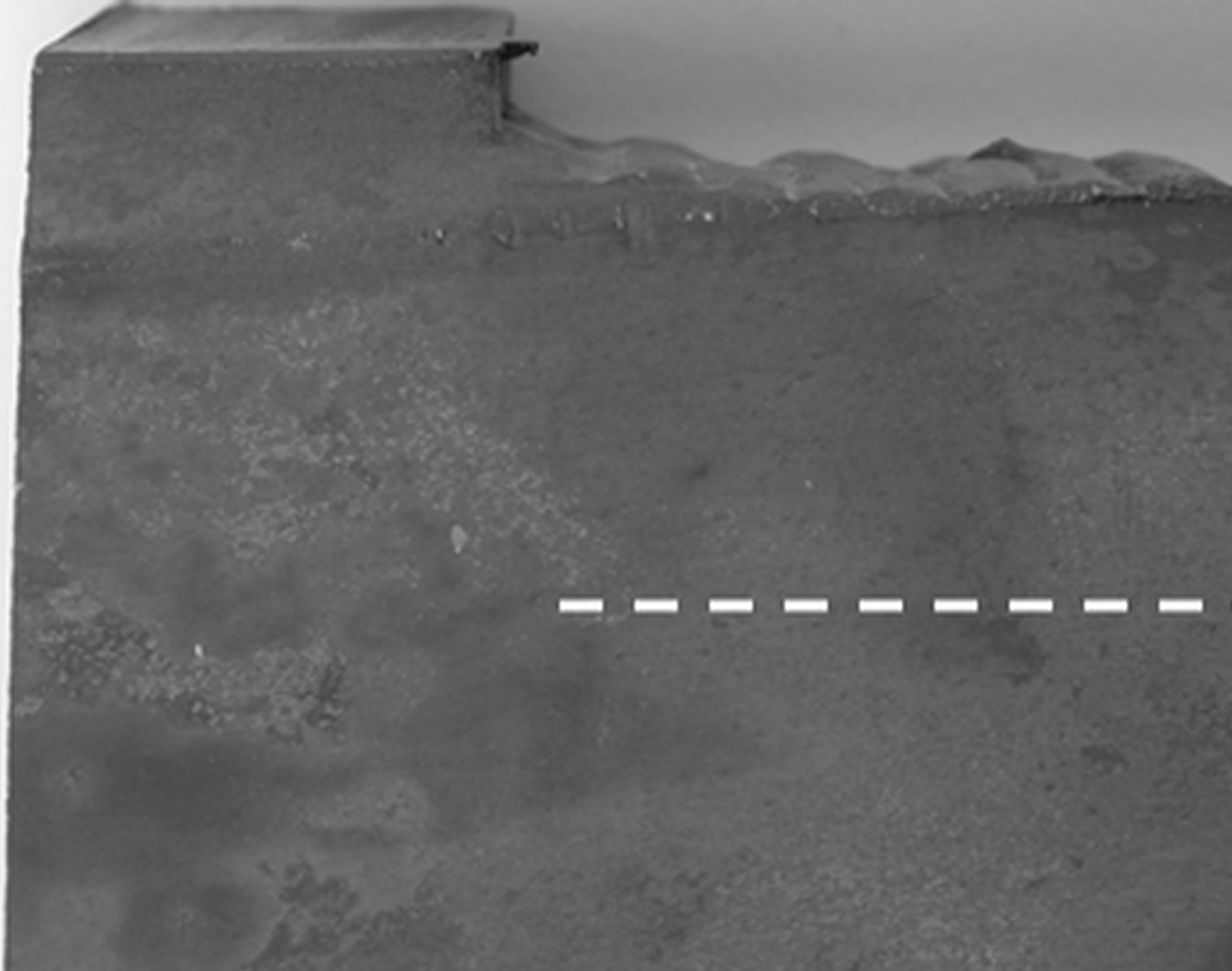

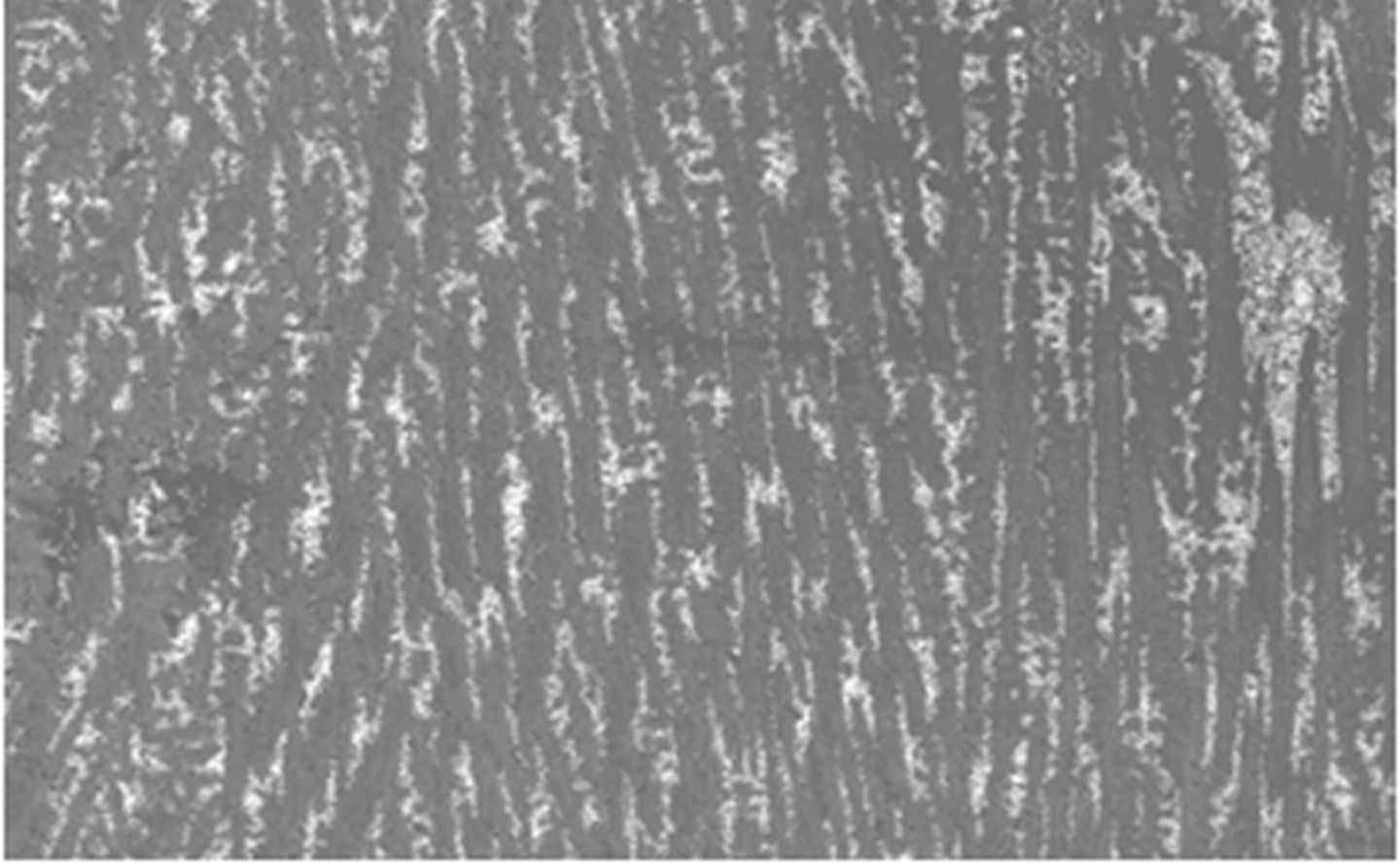

Z

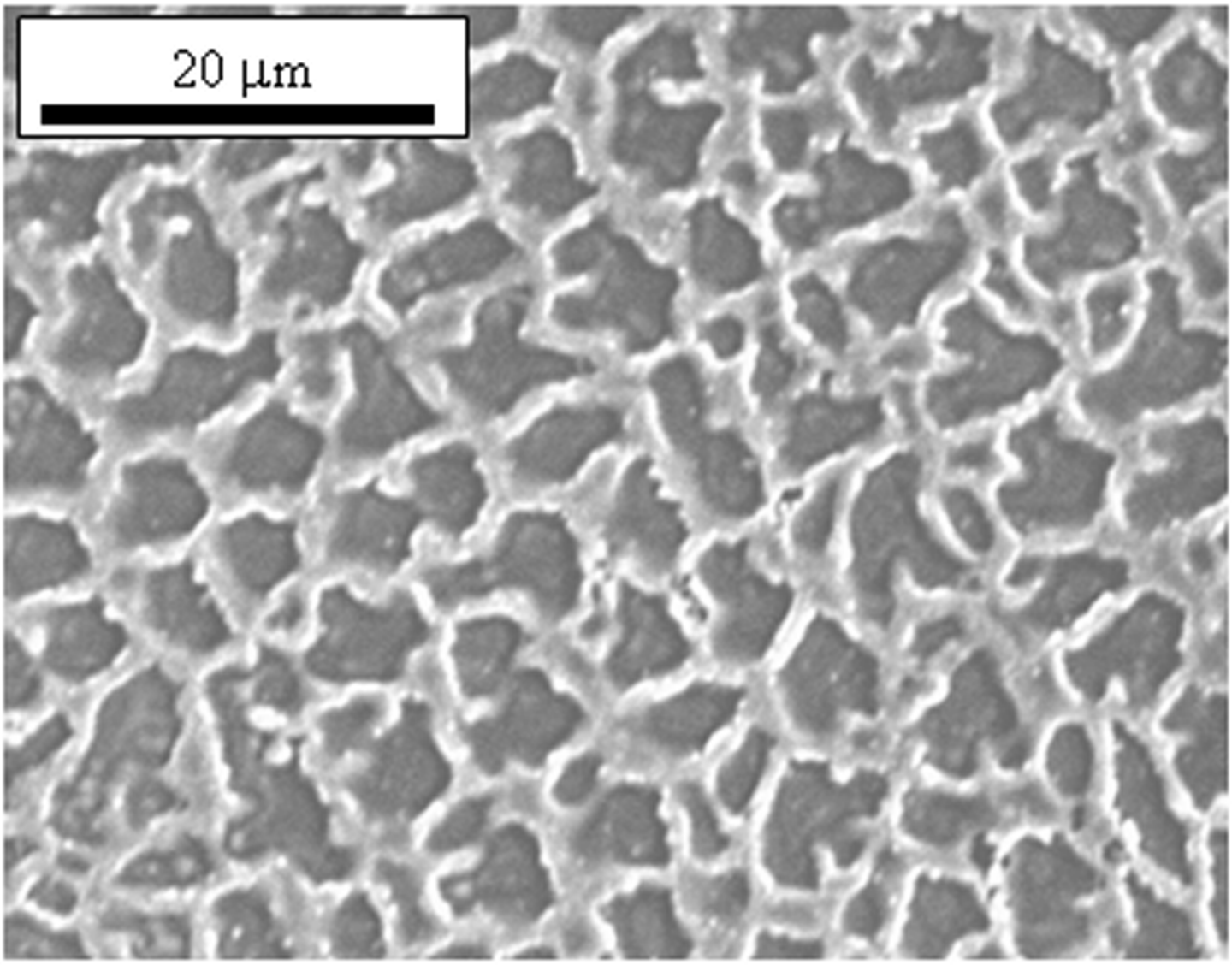

Figure 6

Click here to download high resolution image

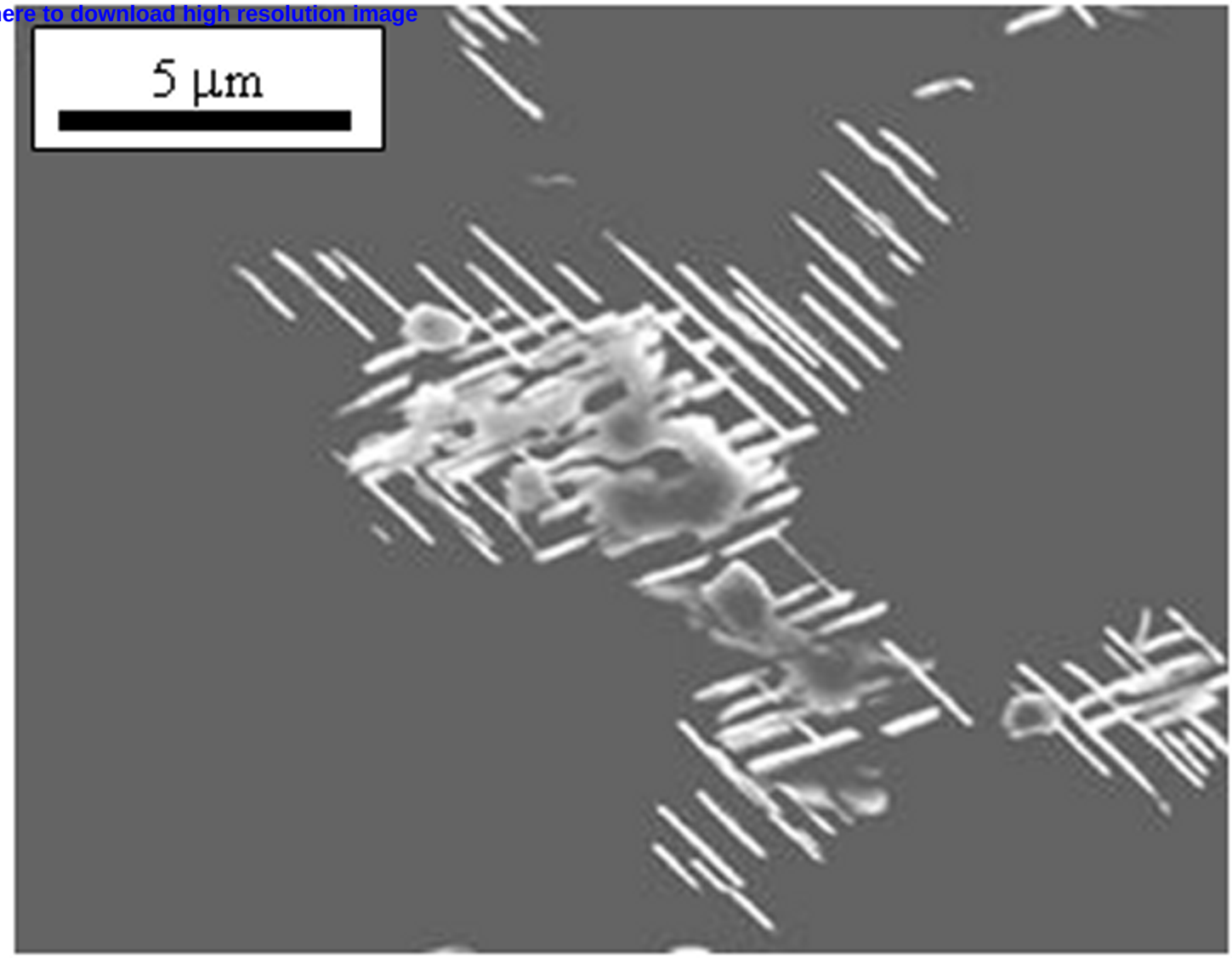

Figure 7

Click here to download high resolution image

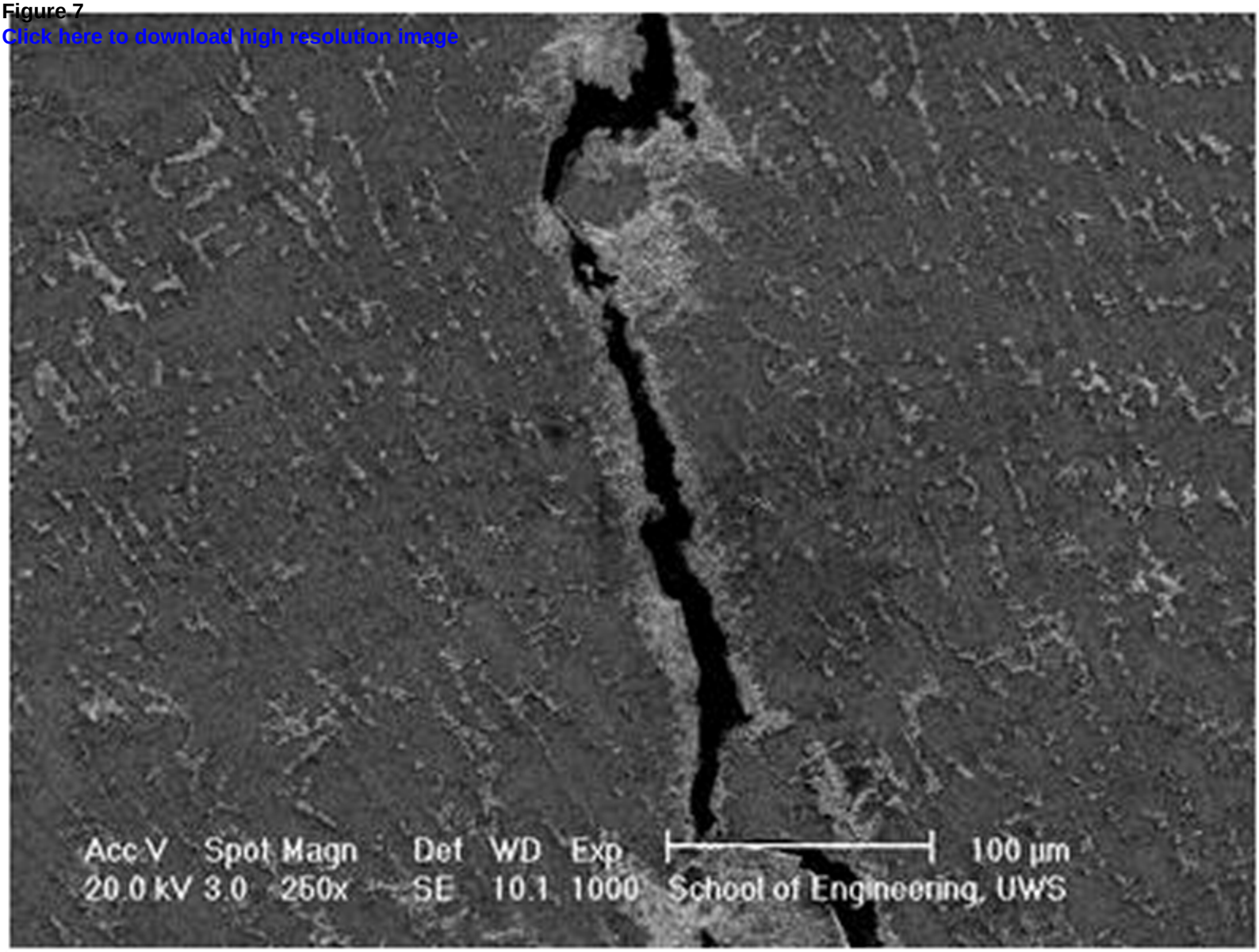

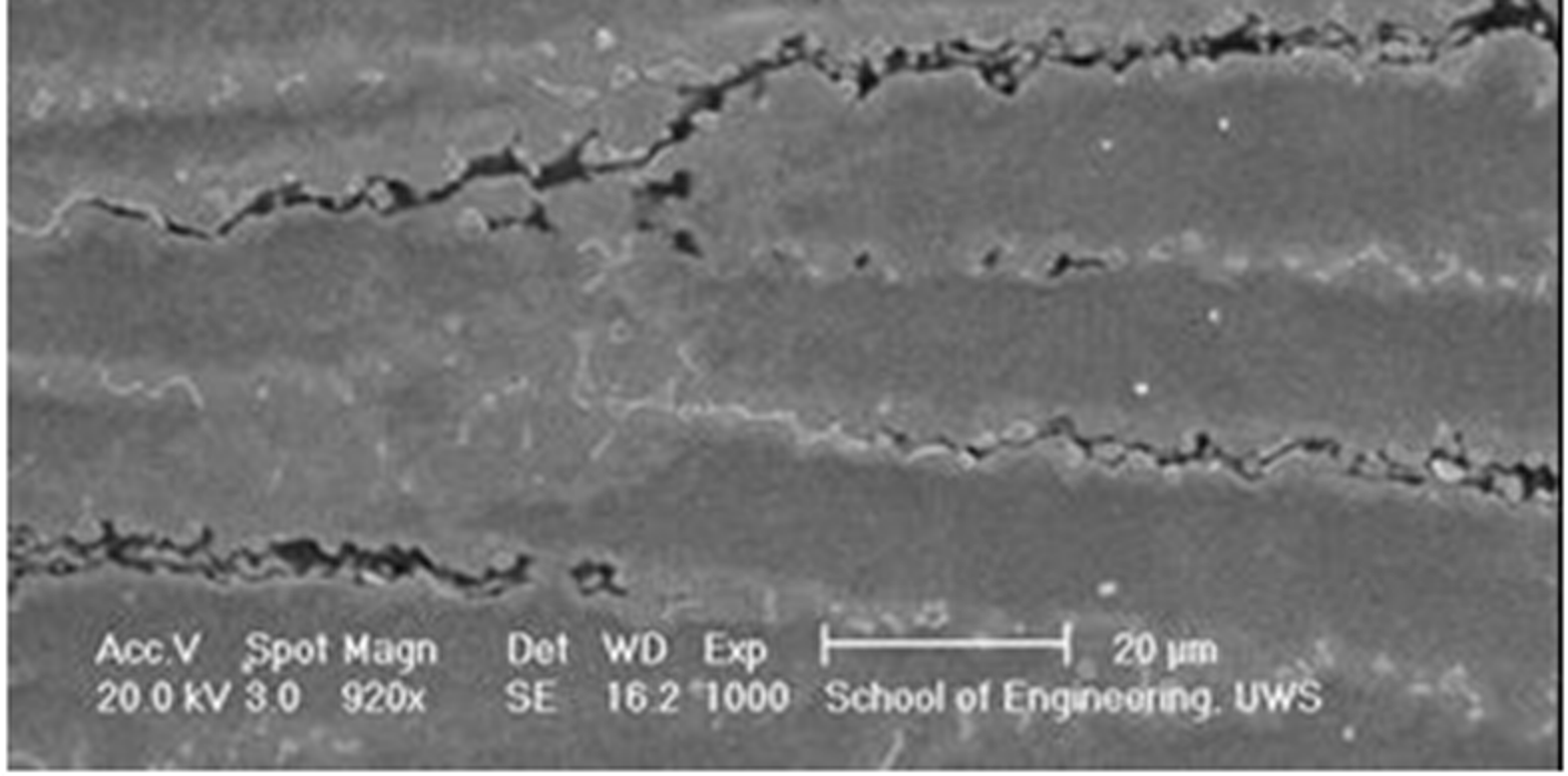
Acc.V Spot Magn Det WD Exp 20 µm
20.0 kV 3.0 920x SE 16.2 1000 School of Engineering, UWS

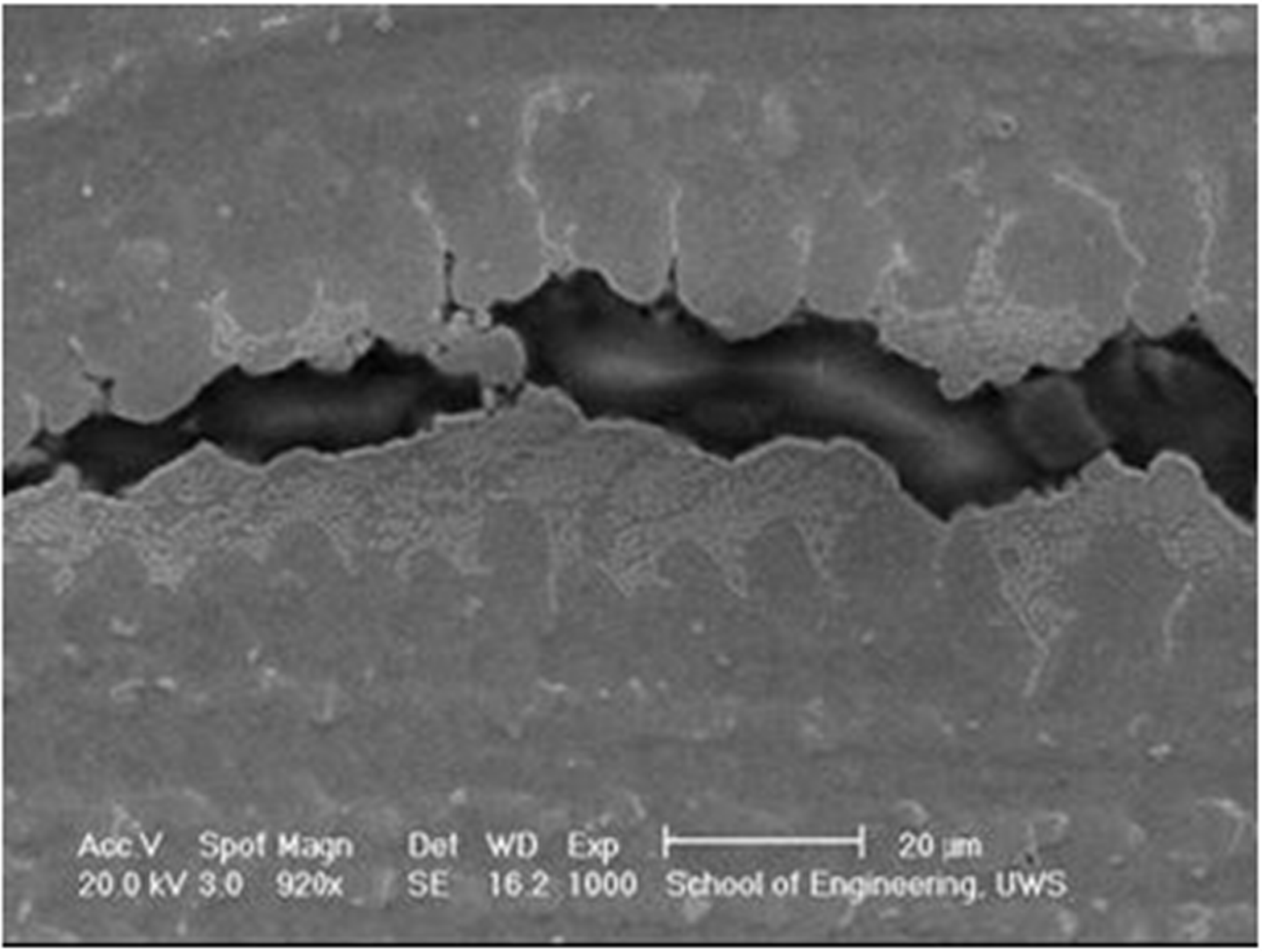
Acc.V Spot Magn Det WD Exp 20 µm
20.0 kV 3.0 920x SE 16.2 1000 School of Engineering, UWS

Figure 9
Click here to download high resolution image

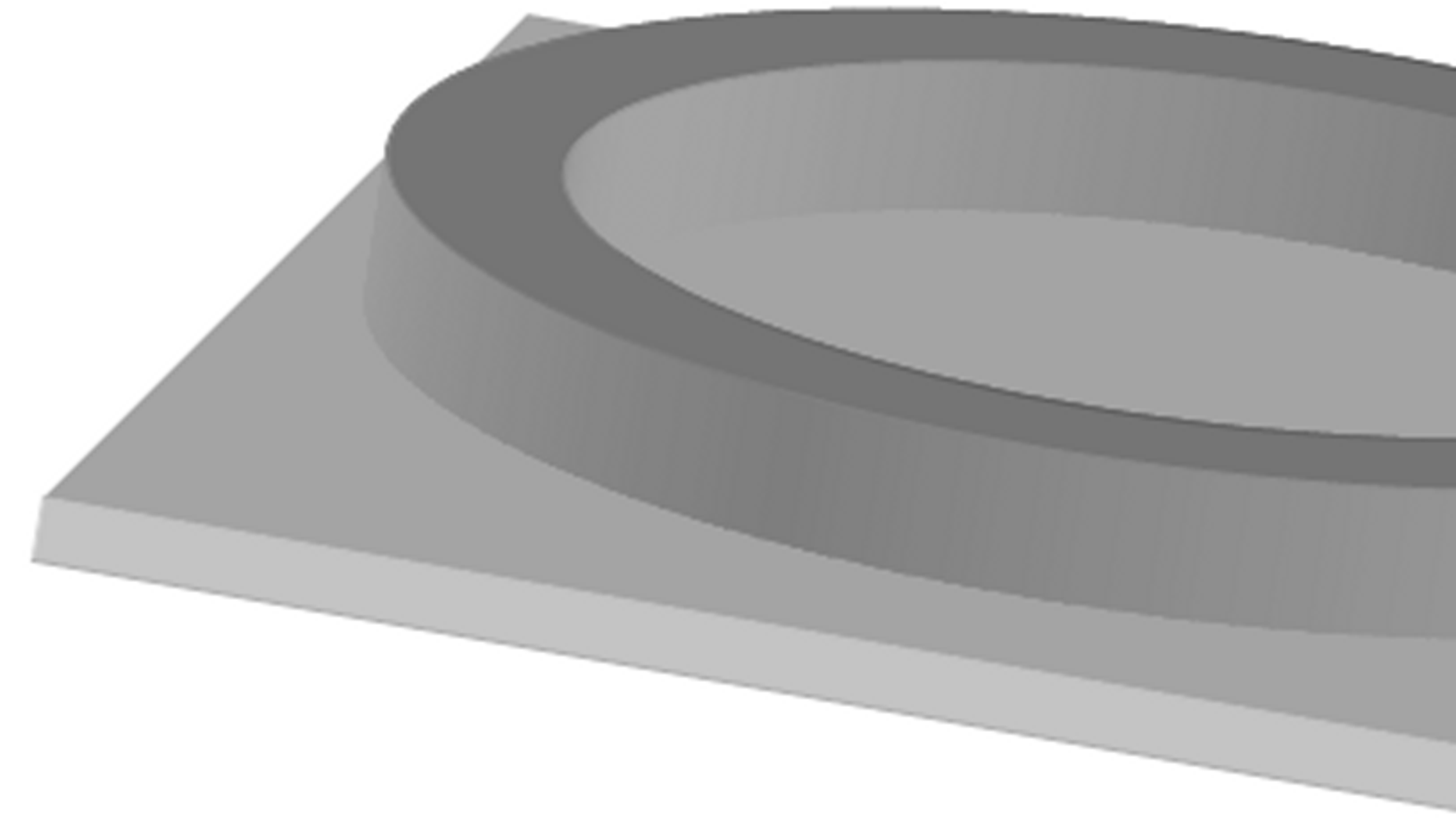

Figure 10

Click here to download high resolution image

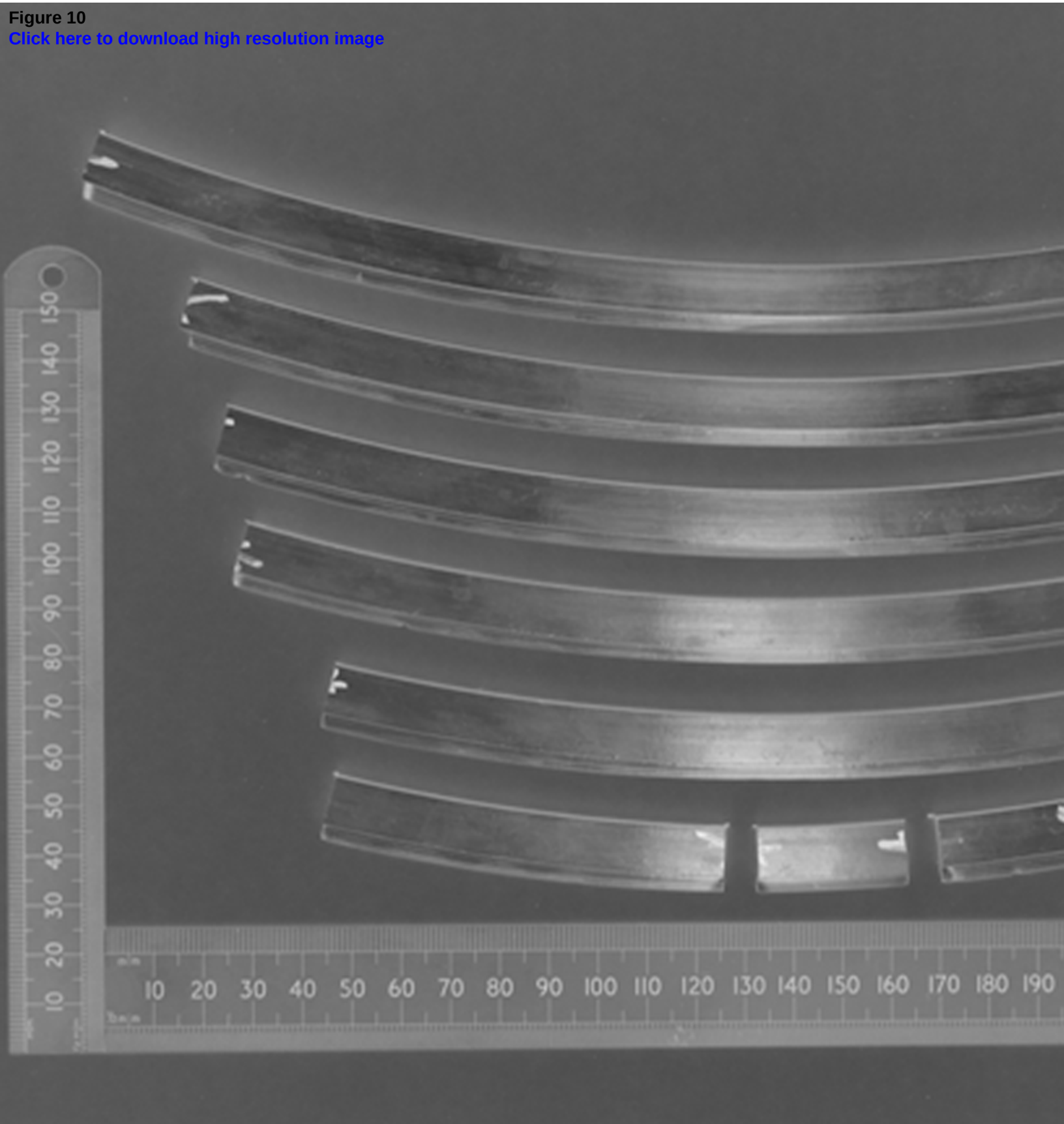

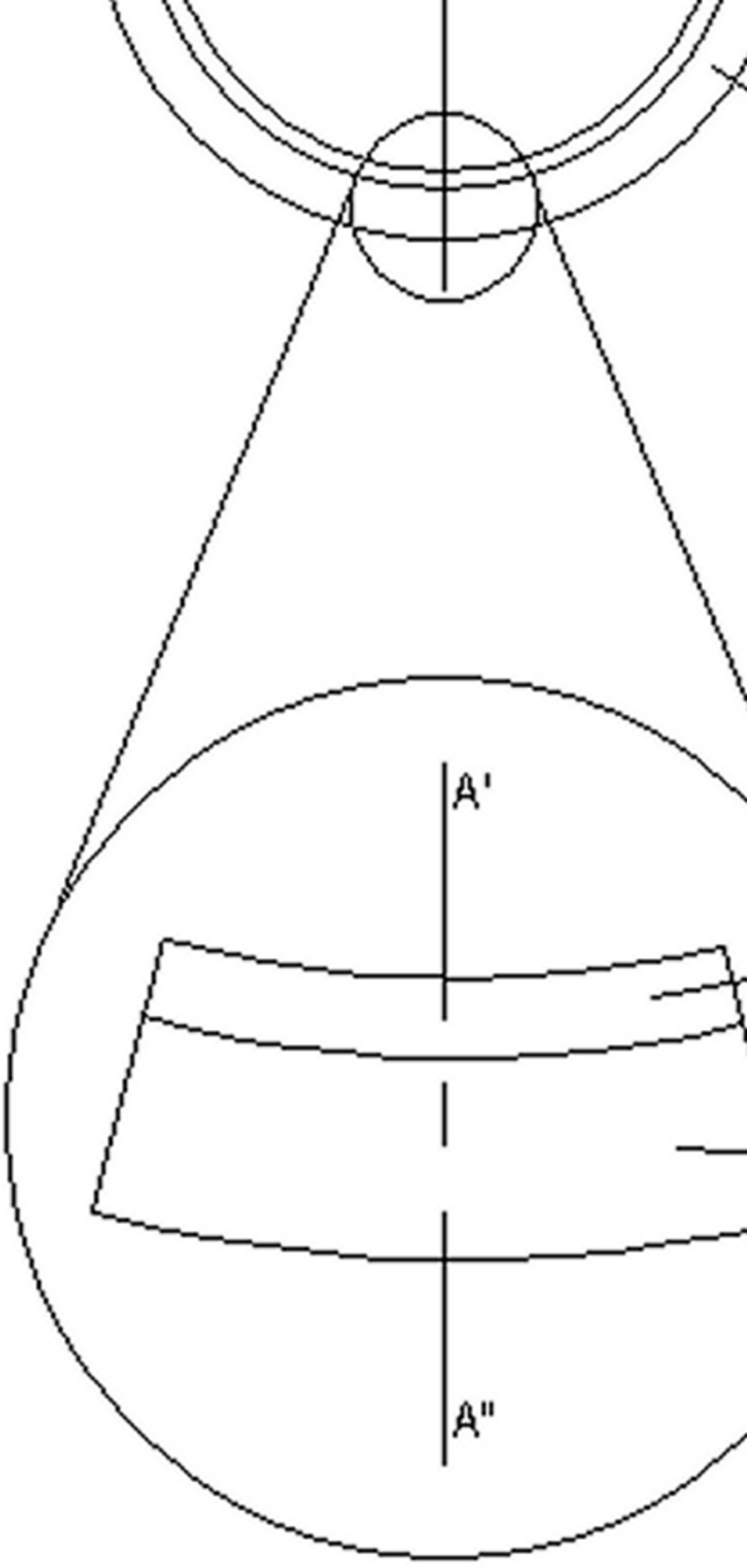
Д'
Д"

(b)

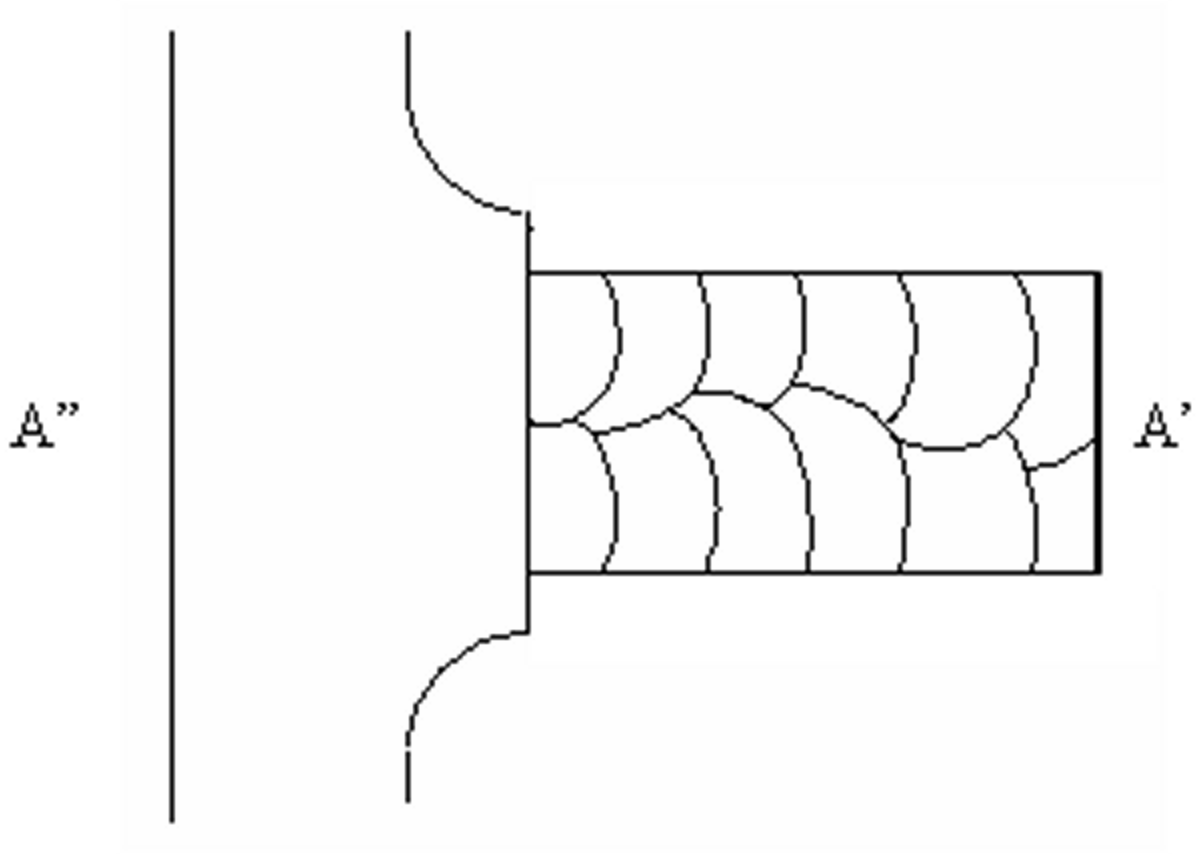

(c)

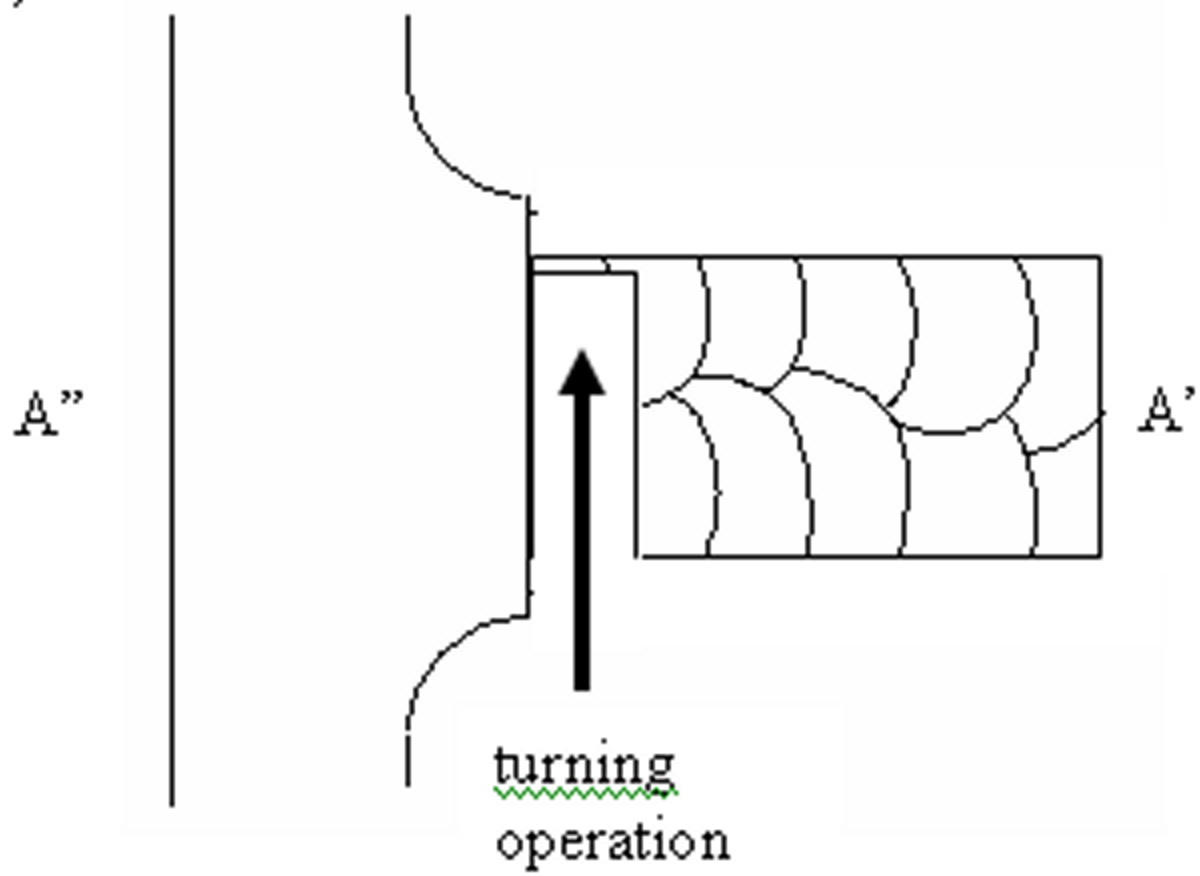

Typical sp

Figure 13
Click here to download high resolution image

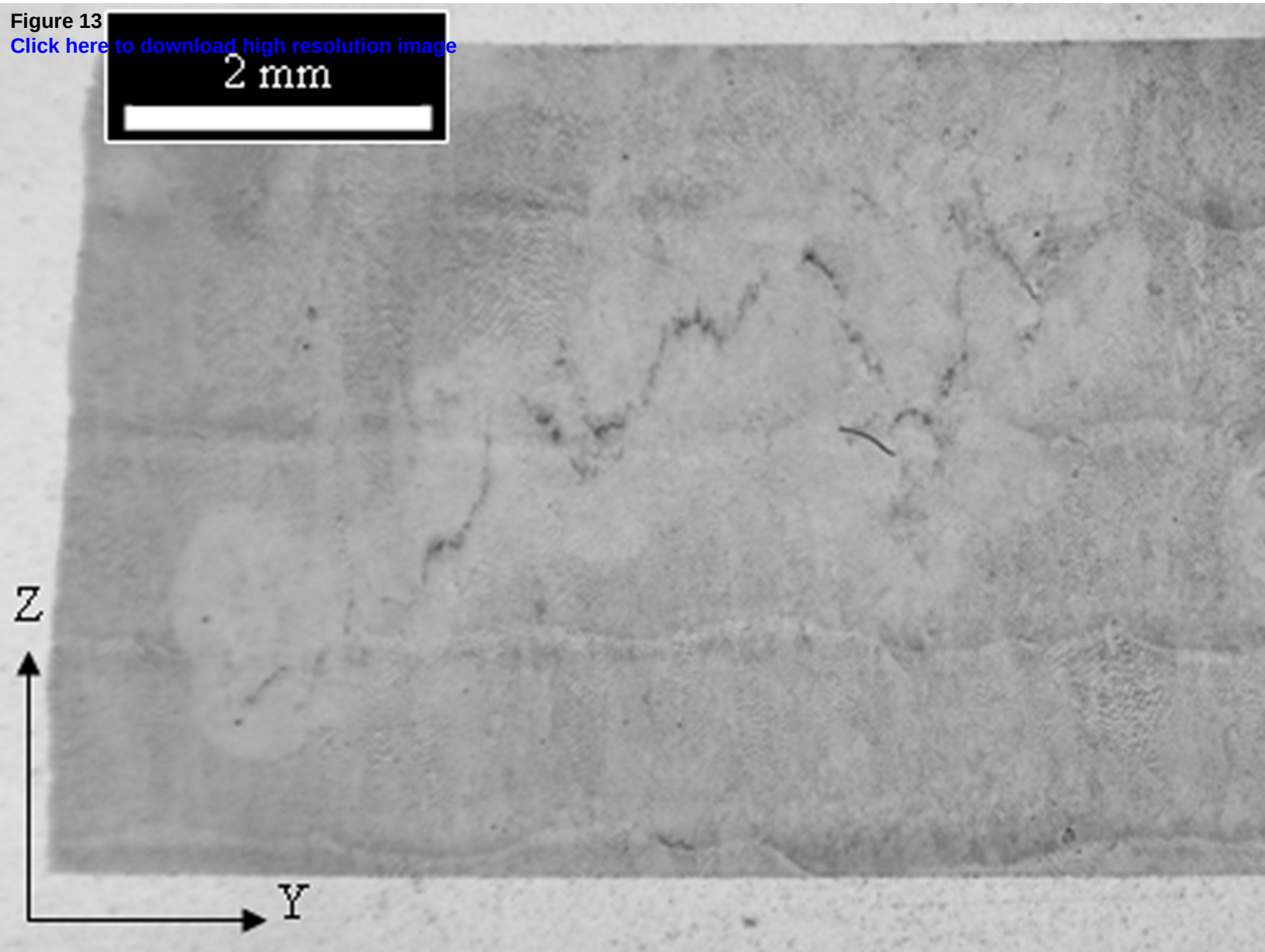

Figure 14

Click here to download high resolution image

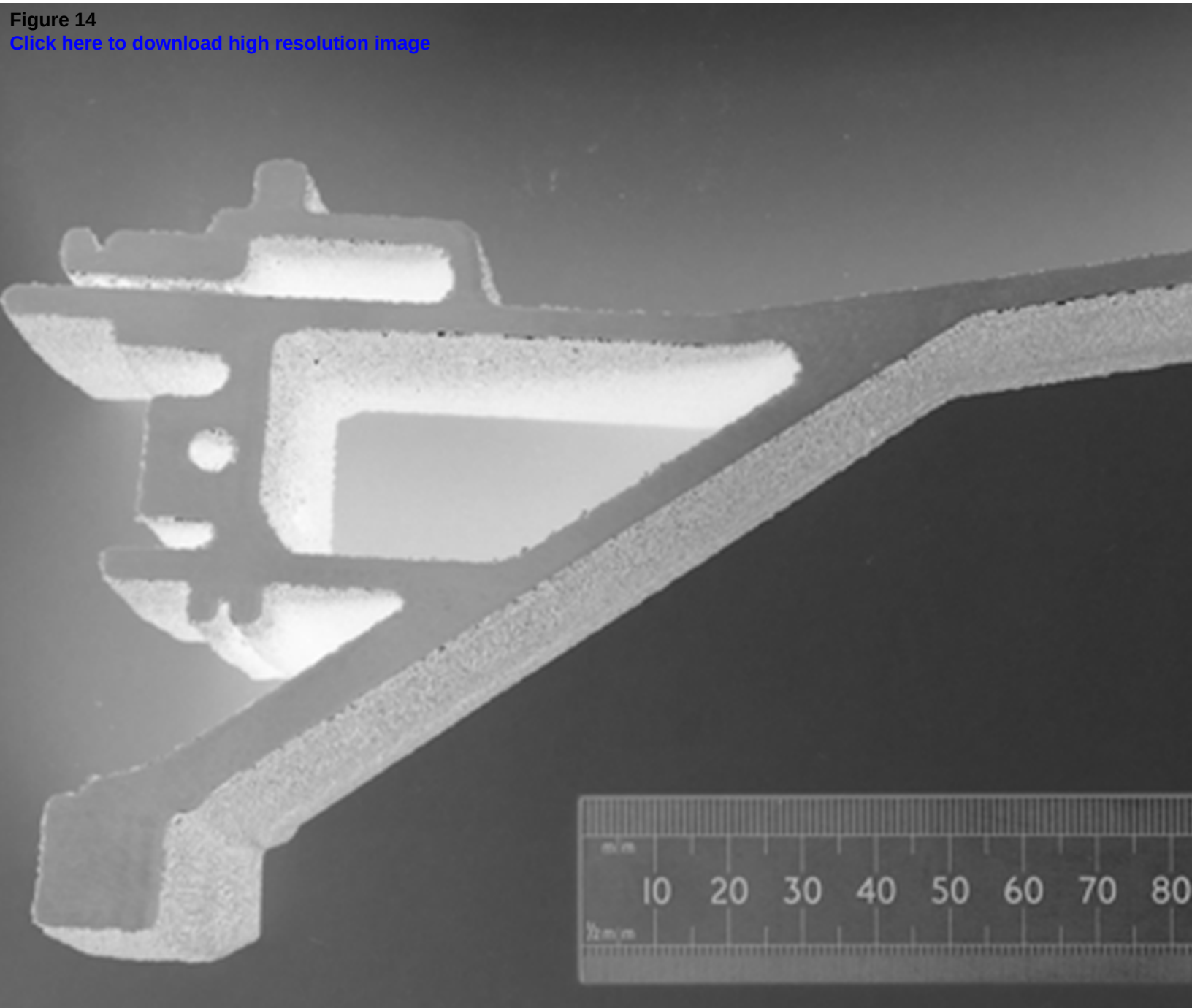

Table 1

Click here to download high resolution image

Voltage [V]	Stickout [mm]	Travel speed [mm/sec]	Wire feed rate [m/min]
35	20	10	10

Table 2

Click here to download high resolution image

Inter-pass temperature	80°C
Welding travel speed	10 mm sec^{-1}
Single bead width	12.8 mm
Single bead height	1.7 mm
Delay time between welds	10 minutes (approx.)

Figure and Table captions

Figure 1. Single stringer / multiple layer depositions.

Figure 2. Schematic definition of weld width (2 x radius), track separation distance, overlap and reference axes (Y axis = direction of deposition).

Figure 3. Double stringer / single layer depositions, showing the overlapping sequence of deposition employed..

Figure 4. An early example of a double stringer / six layer weld illustrated in the X-Z plane. Dashed line represents approximate location, orientation and extent of internal fissures.

Figure 5. Laves phase viewed at relatively low magnification a) micro-stringers parallel to axis of epitaxy (X-Z plane) and b) rafted structure (X-Y plane).

Figure 6. Fine scale δ phase needles in association with laves.

Figure 7. Crack like fissures through dense region of laves precipitation.

Figure 8. Sections through elongated porosity at different locations.

Figure 9. Schematic representation of double stringer / multiple layer SMD cylinders.

Figure 10. Chord sections extracted from the SMD casing flange.

Figure 11. Simplified schematic representation of the combustion casing and internal flange together with three dimensional axis designations (not to scale).

Figure 12. Schematic sections through location A'-A" in Figure 11(a) SMD weld bead lay-up, (b) post flange machining and (c) final specimen extraction operation.

Figure 13. Sinuous cracking viewed after sectioning and etching.

Figure 14. Cross-section of developmental DLD (Direct Laser Deposition) structure in Alloy 718.

Table I. Optimized control parameters for a single pass MIG weld in IN718.

Table II. Nominal SMD weld deposition parameters for fabrication of casing flange.